

Supplementary material for the paper
**'Subduction initiation at an oceanic transform fault
experiencing compression: Role of the fault structure and of
the brittle-ductile transition depth'**

D. Arcay, S. Abecassis, S. Lallemand

Earth and Planetary Science Letters, Volume 618, 2023, 118272, ISSN 0012-821X,
<https://doi.org/10.1016/j.epsl.2023.118272>.

Contents

S1 Additional data: Tables and figures	2
S1.1 Fixed thermomechanical parameters	2
S1.2 Complete simulation list	3
S1.3 Regime diagram of convergence accommodation mode for a thermal transition width $TTW = 30$ km	9
S1.4 Predicted depth of the brittle-ductile transition, z_{BDT} , as a function of lithospheric age	10
S1.5 Comparison between the boundaries of the subduction initiation regime and the depths of the brittle-ductile transition within the 2 converging plates when $TTW = 30$ km	11
S1.6 Regime diagrams for the fault gouge depth expected for subduction initiation at Mussau trench	12
S2 Simulation characterization relative to the modeled tectonic force, F_{res}	12
S3 Analysis of the OP subduction process	15
S4 Failure of convergence localization while z_{wz} is very deep - Influence of TTW	16
S5 Long-term evolution of the tectonic force, F_{res}	16
S6 Additional experiments, investigating different rheologies	19

S1. Additionnal data: Tables and figures

S1.1. Fixed thermomechanical parameters

Table S1: Constant names and values.

Parameter name	Symbol	Value
Box height	H_0	555 km
Bottom temperature	T_b	1888 K
Surface temperature	T_s	273 K
Mantle density at surface	ρ_m^{ref}	3300 kg.m ⁻³
Crust density at surface	ρ_c^{ref}	3300 kg.m ⁻³
Mantle radiogenic heat production	D_0	9.20 × 10 ⁻⁸ W.m ⁻³
Adiabatic gradient	$(\frac{\partial T}{\partial z})_{adiab}$	0.445 K.km ⁻¹
Thermal diffusivity	κ	8 × 10 ⁻⁷ m ² .s ⁻¹
Thermal expansion coefficient	α	3.5 × 10 ⁻⁵ K ⁻¹
Heat capacity	C_p	0.971 × 10 ³ J.(K.kg) ⁻¹
Activation energy for the mantle	E_a^m	465 kJ/mol
Activation energy for the crust	E_a^c	360 kJ/mol
Activation volume	V_a	1.7 × 10 ⁻⁵ m ³ /mol
Pre-exponential factor in non-Newtonian rheology	B_0	339428.7 MPa ⁻³ .s ⁻¹
Dissipation number	$Di = \frac{\alpha g H_0}{C_p}$	0.196
Gravity acceleration	g	9.81 m.s ⁻²
Oceanic crust thickness	h_c	8.325 km
Cohesive strength at $z = 0$	C_0	1 MPa
Yield strength increase with depth for the crust	γ_c	0.05
Yield strength increase with depth for the mantle	γ_m	1.6
Stress exponent in the brittle rheology	n_p	30
Stress exponent in the dislocation creep rheology	n	3
Gas constant	R	8.314 J.(mol. K) ⁻¹
Reference strain rate	$\dot{\varepsilon}_{ref}$	10 ⁻¹⁴ s ⁻¹
Convergence velocity applied on each plate	v_c^{half}	0.5 cm/yr
Reference viscosity at box bottom	ν_{BB}	3.94 × 10 ²⁰ Pa.s

S1.2. Complete simulation list

The complete simulation list is presented as a function of first, increasing young plate age, and, second, increasing old plate age. The first letter in the simulation labelling indicates the thermal transition width, either narrow ('N') and equals to 10 km, or wide ('W') and set to 30 km. The alphabetical tag refers to the weak zone depth at simulation start. 'NL': No deformation localization at the fault gouge. 'OPs': OP subduction initiation. 'YPs': YP subduction initiation. 'SOPs/SYPs': secondary deformation localization at the fault gouge, yielding either YP or OP subduction initiation (section 3.1.4). 'UOPs': unease localization, during which deformation is first partitioned between YP shortening at the left-hand kinematic condition and shortening at the fault gouge, before deformation localizes at the fault gouge and plate underthrusting becomes dominant. 'Double S': both lithospheres are simultaneously subducting. 'O-YPs': OP subduction initiates and aborts, then YP subduction initiates. $\overline{F_{res}}^{\sqrt{t}}$ is the resulting force mean computed on the total simulation duration. 'admis.' and 'too cp': the F_{res} evolution is considered as admissible or excessively compressive, with respect to the considered threshold (see sections 3.3 and S2)). The dash symbol ('-') in columns 10 and 12 means that the considered compressive threshold is never exceeded during the experiment. Otherwise, the overrunning time span is given, followed by the F_{res} mean during this time span. The next columns 11 and 13 indicates how the experiment is then classified with respect to the chosen F_{res} threshold, either showing an admissible evolution of horizontal compressive stresses ('admis.') or an excessively high compression ('too cp'). The experiments that could be considered as leading to an aborted subduction initiation (stop at an early stage, see section S2) are marked with an asterisk in columns 11 and 13 ('too cp*').

Table S2: Complete simulation list.(continued on next pages)

Run name	A_y (Myr)	A_o (Myr)	$\Delta A/A_y$	z_{TT} (km)	TTW z_{wz} (km)	Result	$\overline{F_{res}}^{\sqrt{t}}$ (10^{12} N/m)	If $F_1^{threshold}$ (10^{12} N/m)	Conclusion 1?	If $F_2^{thres} = 15$? (10^{12} N/m)	Conclusion 2?	
N1a	2	5	1.5	35.6	10	8.3	NL	11.3	13.7-30Ma:16.7	too cp	19.7-30.2Ma:18	too cp
N1b	2	5	1.5	35.6	10	9	NL	12.1	27 Ma	too cp	0-15Ma:20	too cp
N1c	2	5	1.5	35.6	10	9.9	SOPs	4.5	-	admis.	-	admis.
N1d	2	5	1.5	35.6	10	11	DS	5.1	-	admis.	-	admis.
N1e	2	5	1.5	35.6	10	11.9	YPs	2.7	-	admis.	-	admis.
N1f	2	5	1.5	35.6	10	14.1	YPs	2.3	-	admis.	-	admis.
N1g	2	5	1.5	35.6	10	16	YPs	2.6	-	admis.	-	admis.
N2a	5	10	1	46.7	10	8.3	NL	12.3	$t > 12$ Ma:16.9	too cp	17.8-28Ma:19.3	too cp
N2b	5	10	1	46.7	10	9.9	NL	19.8	-	too cp	$t > 16.3$ Ma:26	too cp
N2c	5	10	1	46.7	10	11	OPs	6.9	-	admis.	-	admis.
N2d	5	10	1	46.7	10	12.3	OPs	7.4	-	admis.	-	admis.
N2e	5	10	1	46.7	10	14.6	OPs	8.8	-	admis.	-	admis.
N2f	5	10	1	46.7	10	16	DS	10.3	-	admis.	-	admis.
N2g	5	10	1	46.7	10	17.2	YPs	3.6	-	admis.	-	admis.
N2h	5	10	1	46.7	10	24.6	YPs	3.4	-	admis.	-	admis.
N2i	5	10	1	46.7	10	39	YPs	3.2	-	admis.	-	admis.
N3a	5	20	3	54.0	10	12.3	NL	19.6	always exceeded	too cp	$t > 16.9$ Ma: 25	too cp

continued on the next page...

...continued

Run	A_y	A_o	$\Delta A/A_y$	z_{TT}	$TTW z_{wz}$	Result	$F_{res}^{-\sqrt{t}}$	If $F_1^{threshold}$?	Ccls.1?	If $F_2^{threshold}$?	Ccls.2?
N3b	5	20	3	54.0	10	15.4 SOPs	14.1	7-44 Ma:15.9	too cp	18.5-33.7Ma:20.7	too cp
N3c	5	20	3	54.0	10	17.2 SOPs	12.7	11.4-17 Ma:12.1	too cp	21.7-28.5Ma:20.9	too cp
N3d	5	20	3	54.0	10	18.1 SYPs	14.1	9-33Ma:13.5	too cp	18.4-25.8Ma:17.7	too cp
N3e	5	20	3	54.0	10	19 YPs	4.8	-	admis.	-	admis.
N3f	5	20	3	54.0	10	33.1 YPs	4.2	-	admis.	-	admis.
N3g	5	20	3	54.0	10	45 YPs	4.3	-	admis.	-	admis.
N4a	5	30	5	59.1	10	17.2 NL	19.8	8-47Ma:22.4	too cp	$t > 16.8$ Ma: 25	too cp
N4b	5	30	5	59.1	10	19.1 NL	19.7	always exceeded	too cp	$t > 16.6$ Ma:25	too cp
N4c	5	30	5	59.1	10	20.9 SYPs	7.2	7.4-20.2Ma:11.6	too cp	-	admis.
N4d	5	30	5	59.1	10	21.9 YPs	5.5	-	admis.	-	admis.
N4e	5	30	5	59.1	10	24.6 YPs	5.3	-	admis.	-	admis.
N4f	5	30	5	59.1	10	34 YPs	5.2	-	admis.	-	admis.
N4g	5	30	5	59.1	10	58.5 YPs	5.1	-	admis.	-	admis.
N5a	5	55	10	67.7	10	10.4 NL	8.0	-	admis.	-	admis.
N5b	5	55	10	67.7	10	12.3 NL	20.2	always exceeded	too cp	always exceeded	too cp
N5c	5	55	10	67.7	10	16.6 NL	20.1	always exceeded	too cp	always exceeded	too cp
N5d	5	55	10	67.7	10	18.8 NL	18.6	always exceeded	too cp	always exceeded	too cp
N5e	5	55	10	67.7	10	21.1 NL	17.4	always exceeded	too cp	always exceeded	too cp
N5f	5	55	10	67.7	10	23.3 NL	17.2	always exceeded	too cp	16.9-38.3Ma:22.8	too cp
N5g	5	55	10	67.7	10	24.4 SYPs	12.4	6-37Ma:15	too cp	18-29Ma:19.2	too cp
N5h	5	55	10	67.7	10	25.6 UYPs	6.9	6.6-15Ma:11.4	too cp*	-	admis.
N5i	5	55	10	67.7	10	26.7 YPs	6.1	-	admis.	-	admis.
N5j	5	55	10	67.7	10	28.6 YPs	5.9	-	admis.	-	admis.
N5k	5	55	10	67.7	10	41.6 YPs	5.6	-	admis.	-	admis.
N5l	5	55	10	67.7	10	41.6 YPs	5.7	-	admis.	-	admis.
N5m	5	55	10	67.7	10	73.3 YPs	5.5	-	admis.	-	admis.
N6a	5	80	15	73.2	10	12.3 NL	17.7	always exceeded	too cp	$t > 16$ Ma:21.9	too cp
N6b	5	80	15	73.2	10	17.6 NL	18.3	always exceeded	too cp	$t > 16$ Ma:22.6	too cp
N6c	5	80	15	73.2	10	21 NL	13.6	always exceeded	too cp	16-26Ma:19.2	too cp
N6d	5	80	15	73.2	10	24.3 NL	13.6	always exceeded	too cp	16-28Ma:19.4	too cp
N6e	5	80	15	73.2	10	27.7 SYPs	10.9	6-34Ma:14.1	too cp	18.5-25Ma:17	too cp
N6f	5	80	15	73.2	10	29.1 UYPs	7.4	6.4-17.1Ma:11.7	too cp*	-	admis.
N6g	5	80	15	73.2	10	31.4 YPs	6.7	-	admis.	-	admis.
N6h	5	80	15	73.2	10	35.8 YPs	6.3	-	admis.	-	admis.
N6i	5	80	15	73.2	10	47.5 YPs	6.1	-	admis.	-	admis.
N6j	5	80	15	73.2	10	83 YPs	5.7	-	admis.	-	admis.
N7a	10	30	2	65	10	12.3 NL	13.8	always exceeded	too cp	7.3-12Ma:16	too cp
N7b	10	30	2	65	10	20.0 NL	23.8	always exceeded	too cp	always exceeded	too cp
N7c	10	30	2	65	10	22.3 NL	22.8	always exceeded	too cp	always exceeded	too cp
N7d	10	30	2	65	10	23.5 NL	23.1	always exceeded	too cp	always exceeded	too cp
N7e	10	30	2	65	10	24.6 UYPs	16.3	2-41Ma:18	too cp	7.5-33Ma:20.3	too cp
N7f	10	30	2	65	10	26.8 YPs	8.0	2-19Ma:13	too cp	9.8-12Ma:16	admis.
N7g	10	30	2	65	10	28 YPs	7.7	2-18Ma:12	too cp	9.6-11.7Ma:16.1	admis.
N7h	10	30	2	65	10	40 YPs	7.6	2-18Ma:12.7	too cp	9.5-11.4Ma:15.9	admis.

continued on the next page...

...continued

Run	A_y	A_o	$\Delta A/A_y$	z_{TT}	TTW z_{wz}	Result	$F_{res}^{-\sqrt{t}}$	If $F_1^{threshold}$?	Ccls.1?	If $F_2^{threshold}$?	Ccls.2?
N7i	10	30	2	65	10	59.8 YPs	7.8	2-14Ma:12.8	too cp	9.3-11Ma:15.6	admis.
N7j	10	30	2	65	10	68.0 YPs	7.3	2.4-13.9Ma:12.8	too cp	9.3-10.8Ma:15.6	too cp*
N8a	10	55	4.5	73.6	10	14 NL	23.6	1.7-47.5Ma:23.6	too cp	6.0-11.9Ma:25.9	too cp
N8b	10	55	4.5	73.6	10	20 NL	15.6	1.7-19.5Ma:16.3	too cp	6.9-19.5Ma:17.8	too cp
N8c	10	55	4.5	73.6	10	26 NL	23.1	1.7-45.9Ma:23.7	too cp	6.8-45.9Ma:25.1	too cp
N8d	10	55	4.5	73.6	10	29.6 YPs	11.2	1.7-24.4Ma:14.1	too cp	7.0-15.8Ma:16.9	too cp*
N8e	10	55	4.5	73.6	10	82.0 YPs	9.6	1.8-16.6Ma:13.3	too cp	7.1-11.5Ma:16.4	too cp*
N9e	15	80	4.33	83.4	10	14 NL	25.3	0-47.5Ma:25.3	too cp	2.1-47.5Ma:25.9	too cp
N9f	15	80	4.33	83.4	10	20 NL	25.3	0.3-47.5Ma:25.4	too cp	2.1-47.5Ma:25.9	too cp
N9g	15	80	4.33	83.4	10	29.4 NL	24.9	0.3-47.5Ma:25.0	too cp	2.0-47.5Ma:25.4	too cp
N9h	15	80	4.33	83.4	10	33.5 NL	25.4	0.4-47.5Ma:25.5	too cp	2.0-47.5Ma:25.9	too cp
N9i	15	80	4.33	83.4	10	38.2 NL	25.1	0.4-47.5Ma:25.3	too cp	2.0-47.5Ma:25.7	too cp
N9j	15	80	4.33	83.4	10	42 NL	25.2	0.4-47.5Ma:25.3	too cp	2.0-47.5Ma:25.8	too cp
N9k	15	80	4.33	83.4	10	46 NL	25.2	0.4-47.5Ma:25.4	too cp	2.0-47.5Ma:25.8	too cp
N9l	15	80	4.33	83.4	10	50 NL	25.3	0.4-47.5Ma:25.4	too cp	2.0-47.5Ma:25.9	too cp
N9m	15	80	4.33	83.4	10	60 NL	25.0	0.4-43.9Ma:25.1	too cp	2.1-43.9Ma:25.6	too cp
N9n	15	80	4.33	83.4	10	96.0 NL	22.8	0.4-47.5Ma:22.8	too cp	2.1-47.5Ma:23.1	too cp
N10a	20	30	0.5	72.2	10	8.3 NL	-23	0-20Ma:23	too cp	0-20Ma:23	too cp
N10b	20	30	0.5	72.2	10	10.4 NL	25.0	always exceeded	too cp	always exceeded	too cp
N10c	20	30	0.5	72.2	10	12.2 OPs	9.8	0-21Ma:16	too cp	0-10.1Ma:19.7	too cp
N10d	20	30	0.5	72.2	10	14.1 OPs	8.5	0-13Ma:12.8	too cp	0.6-3.1Ma:15.9	too cp
N10e	20	30	0.5	72.2	10	16.0 OPs	8.3	0-12Ma:12.1	too cp	0.7-1.7Ma:15.1	admis.
N10f	20	30	0.5	72.2	10	17.9 OPs	8.7	0.2-10.4Ma:12.0	too cp	0.6-1.9Ma:15.2	admis.
N10g	20	30	0.5	72.2	10	26.3 OPs	10.7	0.4-21.3Ma:17	too cp	0.5-11Ma:20.3	too cp
N10h	20	30	0.5	72.2	10	28.7 YPs	11.6	0-24Ma:17.6	too cp	0.4-15Ma:20	too cp
N10i	20	30	0.5	72.2	10	33.1 YPs	8.2	0-16.5Ma:15.4	too cp	0.4-7.8Ma:18.5	too cp
N10j	20	30	0.5	72.2	10	38.0 YPs	7.9	0-15Ma:15.2	too cp	0.4-6.8Ma:18.4	too cp
N10k	20	30	0.5	72.2	10	46.4 YPs	8.0	0-14.8Ma:15.5	too cp	0.4-6.7Ma:18.4	too cp
N10l	20	30	0.5	72.2	10	48 YPs	7.9	0-14Ma:15.5	too cp	0.6-6.7Ma:18.4	too cp
N10m	20	30	0.5	72.2	10	68.0 YPs	7.8	0.4-14.4Ma:15.5	too cp	0.4-6.7Ma:18.3	too cp
N11a	20	55	1.75	80.9	10	10.4 NL	26.5	always exceeded	too cp	always exceeded	too cp
N11b	20	55	1.75	80.9	10	12.7 NL	25.1	always exceeded	too cp	always exceeded	too cp
N11c	20	55	1.75	80.9	10	18.2 o-YPs	14.6	0-31Ma:19.1	too cp	0.5-21Ma:22	too cp
N11d	20	55	1.75	80.9	10	21.2 OPs	11.1	0.3-29.7Ma:15.3	too cp	0.5-10.3Ma:18.3	too cp
N11e	20	55	1.75	80.9	10	23.7 YPs	11.5	0-25Ma:17.2	too cp	0.4-12.5Ma:21.4	too cp
N11f	20	55	1.75	80.9	10	26.8 NL	26.2	always exceeded	too cp	always exceeded	too cp
N11g	20	55	1.75	80.9	10	29.6 NL	26.7	always exceeded	too cp	always exceeded	too cp
N11h	20	55	1.75	80.9	10	32.7 NL	26.2	always exceeded	too cp	always exceeded	too cp
N11i	20	55	1.75	80.9	10	44.6 NL	25.3	always exceeded	too cp	always exceeded	too cp
N11j	20	55	1.75	80.9	10	56.5 NL	25.4	always exceeded	too cp	always exceeded	too cp
N11k	20	55	1.75	80.9	10	85 NL	25.5	always exceeded	too cp	always exceeded	too cp
N12a	55	80	0.454	100.1	10	8.3 NL	36.4	always exceeded	too cp	always exceeded	too cp
N12b	55	80	0.454	100.1	10	10.4 NL	36.7	always exceeded	too cp	always exceeded	too cp
N12c	55	80	0.454	100.1	10	12.3 OPs	36.2	always exceeded	too cp	always exceeded	too cp

continued on the next page...

...continued

Run	A_y	A_o	$\Delta A/A_y$	z_{TT}	$TTW z_{wz}$	Result	$F_{res}^{-\sqrt{t}}$	If $F_1^{threshold}$?	Ccls.1?	If $F_2^{threshold}$?	Ccls.2?
N12d	55	80	0.454	100.1	10	24.6 OPs	13.3	0-30.2Ma:18.1	too cp	à-20.0Ma:20	too cp
N12e	55	80	0.454	100.1	10	33.6 OPs	13.4	0-27Ma:20	too cp	0-19.8Ma:22.9	too cp
N12f	55	80	0.454	100.1	10	37.2 OPs	14.2	0-28Ma:20.9	too cp	0.1-20.9Ma:24	too cp
N12g	55	80	0.454	100.1	10	38.9 OPs	16.5	0-30Ma:22.8	too cp	0.1-23.3Ma:25.9	too cp
N12h	55	80	0.454	100.1	10	40.5 NL	36.1	always exceeded	too cp	always exceeded	too cp
N12i	55	80	0.454	100.1	10	43.5 NL	36.7	always exceeded	too cp	always exceeded	too cp
N12j	55	80	0.454	100.1	10	45.5 YPs	38.9	0-14.9Ma:38.9	too cp	0.3-14.9Ma:39.4	too cp
N12k	55	80	0.454	100.1	10	47.4 YPs	17.1	0-27Ma:27	too cp	0.3-25.4Ma:28.9	too cp
N12l	55	80	0.454	100.1	10	64.7 YPs	15.9	0-26Ma:26.1	too cp	0.3-24Ma:27.8	too cp
N12m	55	80	0.454	100.1	10	90 YPs	16.0	0-27Ma:25	too cp	0.3-23.7Ma:27.8	too cp
W1a	2	5	1.5	35.6	30	8. NL	12.2	13.8- 35.9Ma:17.7	too cp	19.7-34.6Ma:20.2	too cp
W1b	2	5	1.5	35.6	30	9. NL	12.5	14-47Ma:16.9	too cp	20-34Ma:20.5	too cp
W1c	2	5	1.5	35.6	30	9.8 UOPs	3.5	-	admis.	-	admis.
W1d	2	5	1.5	35.6	30	11 YPs	3.0	-	admis.	-	admis.
W1e	2	5	1.5	35.6	30	14 YPs	2.8	-	admis.	-	admis.
W2a	5	10	1	46.7	30	8.3 NL	12.3	t>12 Ma:16.9	too cp	17.8-28Ma:19.4	too cp
W2b	5	10	1	46.7	30	9.9 NL	19.9	always exceeded	too cp	t >16.3Ma:25.7	too cp
W2c	5	10	1	46.7	30	11 OPs	7.3	-	admis.	-	admis.
W2d	5	10	1	46.7	30	12.3 OPs	7.83	-	admis.	-	admis.
W2e	5	10	1	46.7	30	13.3 OPs	7.1	-	admis.	-	admis.
W2f	5	10	1	46.7	30	14.7 YPs	3.0	-	admis.	-	admis.
W2g	5	10	1	46.7	30	26.7 YPs	3.1	-	admis.	-	admis.
W2h	5	10	1	46.7	30	38.7 YPs	2.7	-	admis.	-	admis.
W3a	5	20	3	54.0	30	12.3 NL	19.6	-	admis.	-	admis.
W3b	5	20	3	54.0	30	15.4 NL	17.2	t >9.6 Ma:19.7	too cp	17-42.4Ma:29.2	too cp
W3c	5	20	3	54.0	30	16.2 YPs	4.7	-	admis.	-	admis.
W3d	5	20	3	54.0	30	17.0 YPs	3.8	-	admis.	-	admis.
W3e	5	20	3	54.0	30	20.4 YPs	3.8	-	admis.	-	admis.
W3f	5	20	3	54.0	30	49.9 YPs	4.0	-	admis.	-	admis.
W4a	5	30	3	59.1	30	12.3 NL	19.5	9-47Ma:22	too cp	17.4-47Ma:25.5	too cp
W4b	5	30	3	59.1	30	17.2 NL	19.7	9.5-47Ma:22.8	too cp	16.2-47Ma:25.2	too cp
W4c	5	30	3	59.1	30	18.4 YPs	5.1	-	admis.	-	admis.
W4d	5	30	3	59.1	30	20.9 YPs	4.6	-	admis.	-	admis.
W4e	5	30	3	59.1	30	33.8 YPs	4.4	-	admis.	-	admis.
W4f	5	30	3	59.1	30	58.5 YPs	4.0	-	admis.	-	admis.
W5a	5	55	10	67.7	30	20.3 NL	10.6	6-18Ma:	too cp		
W5b	5	55	10	67.7	30	22.5 YPs	5.8	-	admis.	-	admis.
W5c	5	55	10	67.7	30	25.6 YPs	5.5	-	admis.	-	admis.
W5d	5	55	10	67.7	30	72.7 YPs	4.7	-	admis.	-	admis.
W6a	5	80	15	73.2	30	12.3 NL	19.1	9-47Ma:21.7	too cp	17.2-47Ma:24.3	too cp
W6b	5	80	15	73.2	30	17.6 NL	19.4	8.6-47Ma:22	too cp	16.4-47Ma:24.4	too cp
W6c	5	80	15	73.2	30	21 NL	18.2	6-47Ma:20	too cp	16.1-47Ma:22.4	too cp
W6d	5	80	15	73.2	30	24.0 UYPs	10.3	6-20Ma:11.7	too cp	-	admis.

continued on the next page...

...continued

Run	A_y	A_o	$\Delta A/A_y$	z_{TT}	TTW z_{wz}	Result	$F_{res}^{-\sqrt{t}}$	If $F_1^{threshold}?$	Ccls.1?	If $F_2^{threshold}?$	Ccls.2?
W6e	5	80	15	73.2	30	27.7 YPs	5.8	-	admis.	-	admis.
W6f	5	80	15	73.2	30	82 YPs	5.5	-	admis.	-	admis.
W7a	10	30	2	65	30	12.3 NL	23.9	always exceeded	too cp	always exceeded	too cp
W7b	10	30	2	65	30	15.4 NL	24.0	always exceeded	too cp	always exceeded	too cp
W7c	10	30	2	65	30	17.0 OPs	7.2	3-11.7:12.9	too cp	$\Delta t_{excess} < 1 \text{ Ma}$, 15.3	admis.
W7d	10	30	2	65	30	20.0 NL	12.9	$t > 14 \text{ Ma}:14.6$	too cp	33.8-37.5Ma:15.7	admis.
W7e	10	30	2	65	30	22.0 YPs	7.5	2-17Ma:12.6	too cp	9.0-11.0Ma:15.8	admis.
W7f	10	30	2	65	30	24.0 YPs	6.6	2.5-5.8Ma:10.9	too cp*	6.1-11.7Ma:12.1	admis.
W7g	10	30	2	65	30	28 YPs	6.6	2.5-5.8Ma:10.9	too cp*	6.1-11.7Ma:12.1	admis.
W7h	10	30	2	65	30	59.1 YPs	7.0	2.5-5.8Ma:10.9	too cp*	6.1-12Ma:-12.1	admis.
W8i	10	55	4.5	73.6	30	14 NL	23.6	1.6-47.5Ma:24.1	too cp	6.7-12.3Ma:16.1	too cp
W8j	10	55	4.5	73.6	30	20 NL	23.4	1.6-19.5Ma:24.0	too cp	6.7-12.4Ma:16.1	too cp
W8k	10	55	4.5	73.6	30	23.7 NL	23.2	1.6-45.9Ma:23.7	too cp	6.8-45.9Ma:25.1	too cp
W8l	10	55	4.5	73.6	30	29.6 NL	23.2	1.6-47.5Ma:23.7	too cp	6.8-47.5Ma:25.1	too cp
W8m	10	55	4.5	73.6	30	33.9 YPs	8.5	1.7-11.4Ma:13.1	too cp	8.3-10.1Ma:15.9	admis.
W8n	10	55	4.5	73.6	30	82.0 YPs	9.2	1.8-19.3Ma:12.3	too cp	8.4-10.6Ma:16.3	too cp*
W9a	15	80	4.33	83.4	30	14 NL	24.9	0-47.5Ma:24.9	too cp	1.9-47.5Ma:25.3	too cp
W9b	15	80	4.33	83.4	30	20 NL	25.6	0.3-47.5Ma:25.7	too cp	1.9-47.5Ma:26.1	too cp
W9c	15	80	4.33	83.4	30	26.8 NL	22.3	0.3-47.5Ma:22.5	too cp	2.0-31.6Ma:22.5	too cp
W9d	15	80	4.33	83.4	30	33.5 YPs	13.3	0.4-21.4Ma:15.1	too cp	2.1-11.7Ma:18.5	too cp
W9e	15	80	4.33	83.4	30	38.2 YPs	12.9	0.4-23.1Ma:15.0	too cp	2.1-11.7Ma:18.7	too cp
W9f	15	80	4.33	83.4	30	YPs	9.9	0.4-21.8Ma:21.4	too cp	2.1-12.0Ma:18.9	too cp
W10a	20	30	0.5		30	10.4 NL	24.9	0.5-47.5Ma:24.9	too cp	0.5-47.5Ma:24.9	too cp
W10b	20	30	0.5	72.2	30	12.2 OPs	9.9	0-20.8Ma:15.4	too cp	0-9.6Ma:19.4	too cp
W10c	20	30	0.5	72.2	30	15.9 OPs	7.2	0-8.4Ma:11.4	too cp	-	admis.
W10d	20	30	0.5	72.2	30	17.9 OPs	8.2	0.3-10.3Ma:10.9	too cp	-	admis.
W10e	20	30	0.5	72.2	30	24.0 OPs	10.4	0-17Ma:16	too cp	0.5-9.1Ma:19	too cp
W10f	20	30	0.5	72.2	30	25.0 YPs	13.7	0-26Ma:19	too cp	0.5-18.7Ma:21.8	too cp
W10g	20	30	0.5	72.2	30	30.4 YPs	7.4	0-13Ma:15.0	too cp	0.5-5.6Ma:17.9	too cp
W10h	20	30	0.5	72.2	30	37.6 YPs	7.3	0-11Ma:15.2	too cp	0.6-5.4Ma:17.8	too cp
W10i	20	30	0.5	72.2	30	50.3 YPs	7.2	0-11Ma:15.1	too cp	0.6-5.4Ma:17.8	too cp
W10j	20	30	0.5	72.2	30	63.1 YPs	7.7	0-12Ma:15	too cp	0.6-5.3Ma:17	too cp
W10k	20	30	0.5	72.2	30	68.0 YPs	7.3	0.4-11.9Ma:14.9	too cp	0.6-5.3Ma:15.1	too cp
W11a	20	55	1.75	80.9	30	10.4 NL	26.5	always exceeded	too cp	always exceeded	too cp
W11b	20	55	1.75	80.9	30	12.7 NL	25.1	always exceeded	too cp	always exceeded	too cp
W11c	20	55	1.75	80.9	30	18.2 OPs	15.4	0-40Ma:17.0	too cp	0.5-16.9Ma:19.9	too cp
W11d	20	55	1.75	80.9	30	21.2 OPs	12.1	0-21Ma:10.7	too cp	0.4-12Ma:20	too cp
W11e	20	55	1.75	80.9	30	23.7 NL	11.5	0-25Ma:25.3	too cp	always exceeded	too cp
W11f	20	55	1.75	80.9	30	29.6 UYPs	14.3	0-30Ma:19	too cp	0.4-20.3Ma:21.6	too cp
W11g	20	55	1.75	80.9	30	31.5 YPs	12.7	0.3-28.7Ma:17.1	too cp	0.4-14.1Ma:21.9	too cp
W11h	20	55	1.75	80.9	30	32.5 YPs	12.5	0.3-27.5Ma:17.2	too cp	0.4-13.8Ma:21.9	too cp
W11i	20	55	1.75	80.9	30	34.0 YPs	12.5	0.3-26.7Ma:17.3	too cp	0.4-13.9Ma:21.9	too cp
W11j	20	55	1.75	80.9	30	38.1 YPs	12.2	0-26Ma:17.7	too cp	0.4-14Ma:21.9	too cp
W11k	20	55	1.75	80.9	30	85.0 YPs	12	0.4-27.3Ma:17.5	too cp	0.4-14Ma:21.9	too cp

continued on the next page...

...continued

Run	A_y	A_o	$\Delta A/A_y$	z_{TT}	$TTWz_{wz}$	Result	$F_{res}^{\sqrt{t}}$	If $F_1^{threshold}$?	Ccls.1?	If $F_2^{threshold}$?	Ccls.2?
W12a	55	80	0.454	100.1	30	10.4 NL	36.6	always exceeded	too cp	always exceeded	too cp
W12b	55	80	0.454	100.1	30	12.3 OPs	19.9	0-32Ma:26	too cp	0-27Ma:28.6	too cp
W12c	55	80	0.454	100.1	30	17.9 OPs	14.6	0-32.9Ma:18.9	too cp	0-22.7Ma:21.5	too cp
W12d	55	80	0.454	100.1	30	24.6 OPs	12.2	0-26Ma:19.5	too cp	0-18.6Ma:21.9	
W12e	55	80	0.454	100.1	30	33.6 OPs	36.2	0.5-29.7Ma:20.4	too cp	0-20.6Ma:24	too cp
W12f	55	80	0.454	100.1	30	37.2 NL	36.2	always exceeded	too cp	always exceeded	too cp
W12g	55	80	0.454	100.1	30	38.3 NL	41.4	0-15.6Ma:41.4	too cp	0-15.6Ma:41.4	too cp
W12h	55	80	0.454	100.1	30	39.3 YPs	40.2	0-15.2Ma:40.2	too cp	0-15.2Ma:40.2	too cp
W12i	55	80	0.454	100.1	30	40.5 YPs	17.4	0-27Ma:28	too cp	0-25.6Ma:29.2	too cp
W12j	55	80	0.454	100.1	30	47.4 YPs	16.3	0-27Ma:26	too cp	0.2-24.2Ma:28	too cp
W12k	55	80	0.454	100.1	30	96.0 YPs	15.2	0-26Ma:25.9	too cp	0.3-23.7Ma:27.8	too cp

S1.3. Regime diagram of convergence accommodation mode for a thermal transition width $TTW = 30 \text{ km}$

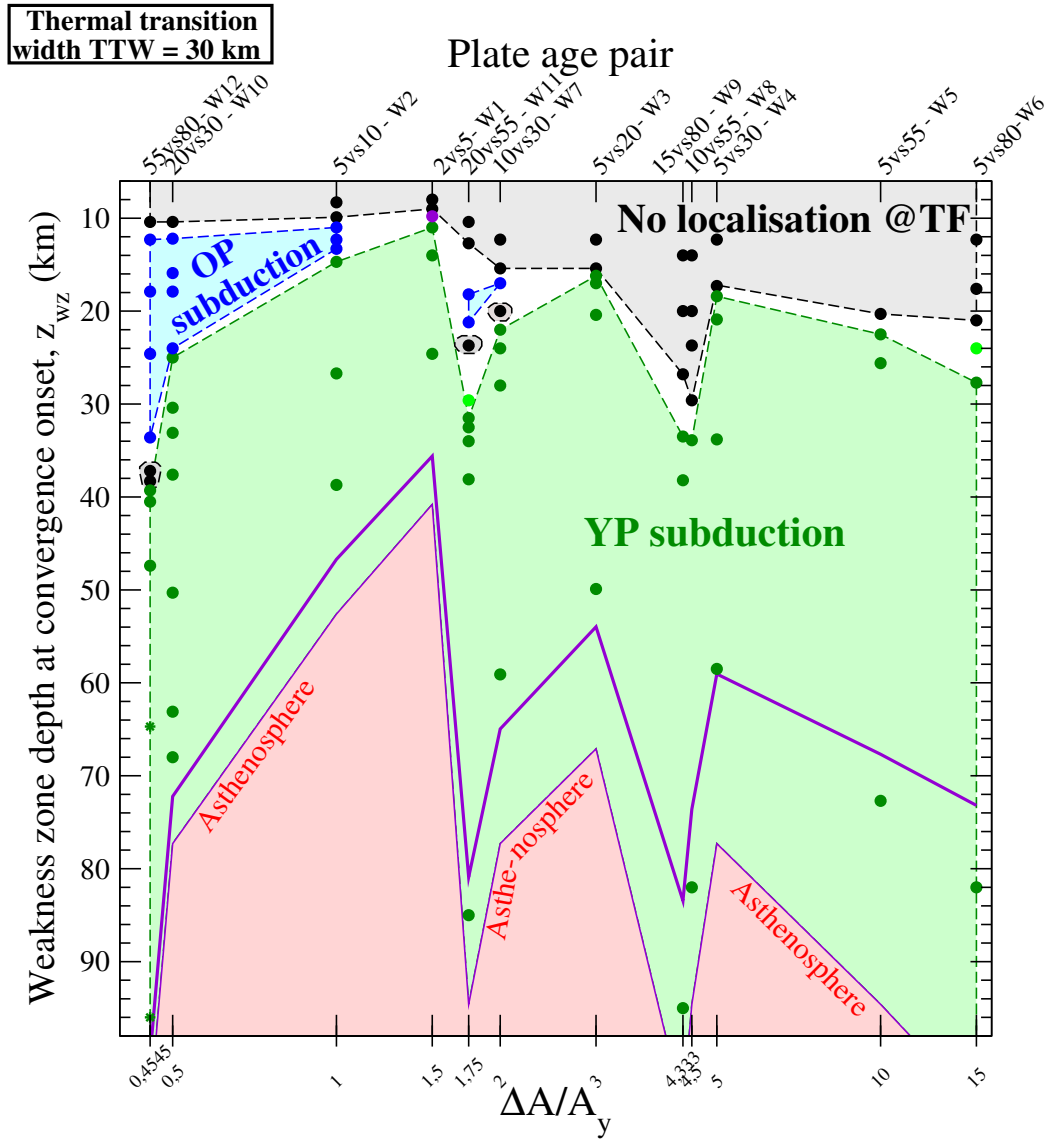


Figure S1: Regime diagram of convergence modes for $TTW=30 \text{ km}$. Simulation results (circles) are depicted as a function of the plate age pair, represented by the parameter $\Delta A/A_y$, and the depth of the weak fault zone imposed at the start of convergence, z_{wz} . The tags of plate age pairs refers to the labelling described in the caption of Table S2. The two purple lines depict, respectively, the depth of the old lithosphere base (1250°C isotherm, thin line), and the reference depth within the thermal transition, z_{TT} (thick line). See Fig. 4 for the legend.

S1.4. Predicted depth of the brittle-ductile transition, z_{BDT} , as a function of lithospheric age

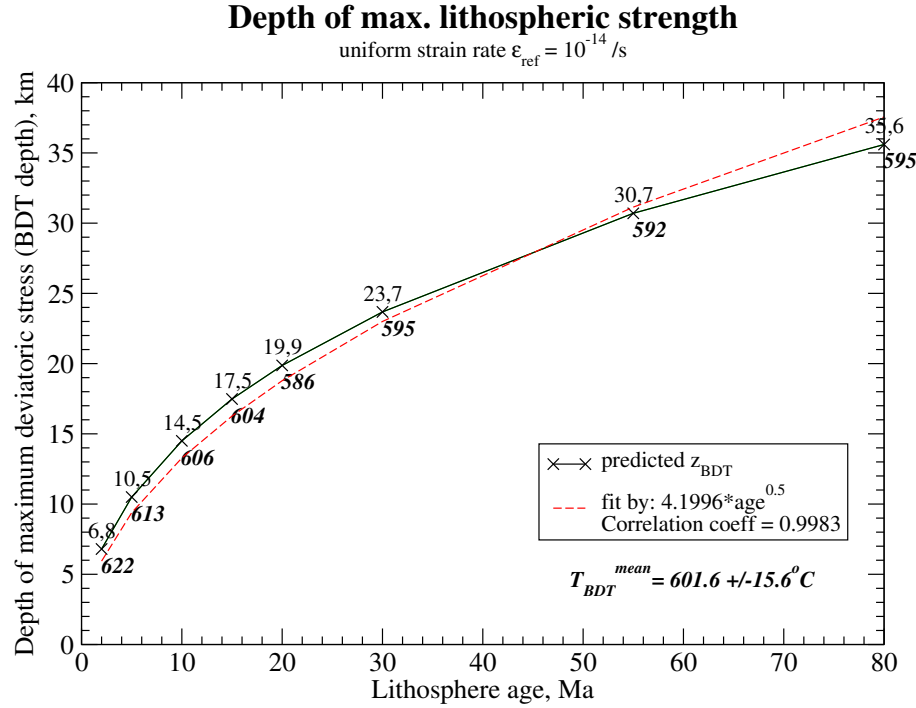


Figure S2: Depth of maximum lithospheric strength, corresponding in our rheological model to the brittle-transition depth, z_{BDT} , as a function of the lithospheric age. The stress profile used to estimate z_{BDT} is computed for the vertical geotherm of a given lithosphere age, using the combined rheology described in section 2.1 and the thermo-mechanical constants in Table S1, assuming a uniform strain rate equal to 10^{-14}s^{-1} (see Fig. 4c). The temperature observed at $z = z_{BDT}$ for the different lithosphere ages (crosses) is indicated in bold and italic.

S1.5. Comparison between the boundaries of the subduction initiation regime and the depths of the brittle-ductile transition within the 2 converging plates when TTW =30 km

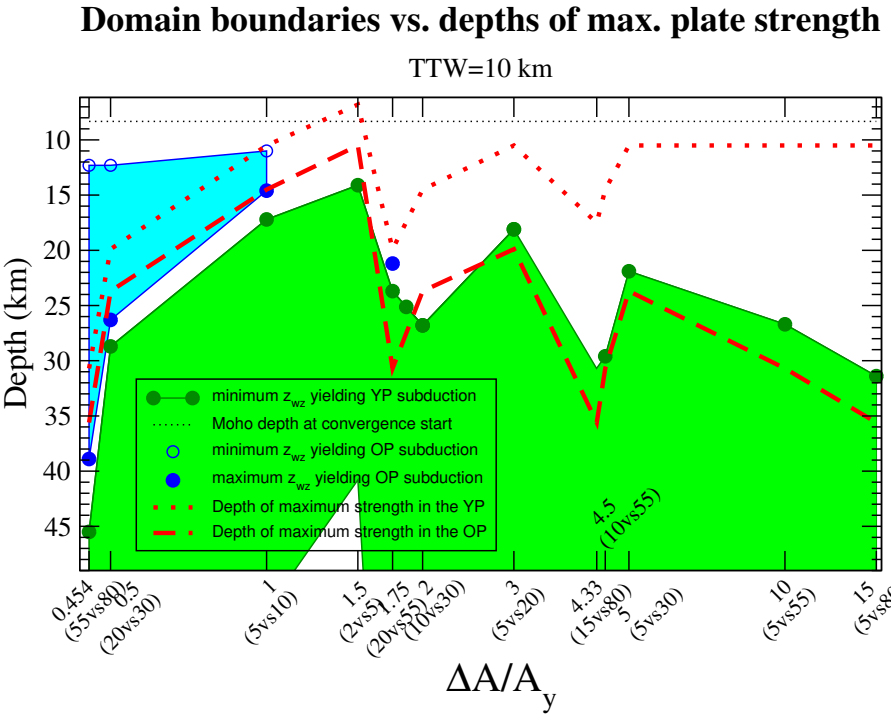


Figure S3: Comparison between the limits of the two subduction domains, in terms of initial fault gouge depth z_{wz} , and the depths of maximum strength, z_{BDT} (defined in Fig. 4c and S3) within both lithospheres at convergence onset for each tested pair of plate ages.

S1.6. Regime diagrams for the fault gouge depth expected for subduction initiation at Mussau trench

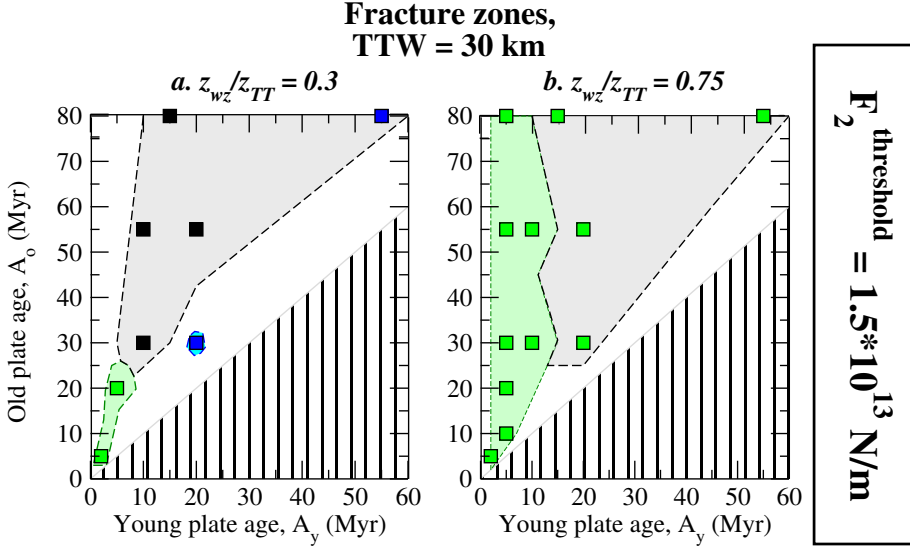


Figure S4: Regime diagrams of convergence accommodation as a function of the two plate ages A_y and A_o , by considering both the obtained deformation style and the evolution of the horizontal tectonic force. The thermal transition widths, TTW , is set to 30 km. The ratio of the weak fault gouge depth to the thermal transition reference depth z_{wz}/z_{TT} is set to 0.3 (a) and 0.75 (b). The threshold defining admissible compressive stresses used to outline the realistic realms of subduction initiation is set to $F_2^{threshold} = 1.5 \times 10^{13} \text{ N/m}$. See Fig. 6 for the legend.

S2. Simulation characterization relative to the modeled tectonic force, F_{res}

The horizontal tectonic force F_{res} that would be necessary to sustain the kinematic boundary conditions applied on both lithospheres (constant plate velocity) is computed for all experiments, as summed up in section 3.3. F_{res} is calculated as the departure from hydrostatic stresses in a reference oceanic column of density $\rho_{ref}(z)$ (?):

$$F_{res} = - \int_0^{z_c} \sigma_{xx} dz + \int_0^{z_c} \rho_{ref}(z) g z dz \quad (1)$$

where σ_{xx} is the horizontal normal component of the stress tensor and z_c is the compensation depth (273 km). F_{res} is estimated at the abscissa either $x = 1027, 1127$, or 1674 km (Fig. 1), to verify that the computation location does not affect the result, except when the forming subduction plane passes at the computational point.

The simulated resulting force has to be compared to the order of magnitude expected on Earth, for which an uncertainty remains. As explained in section 3.3, we consider 2 different values of the admissible threshold, $F_1^{threshold}$ and $F_2^{threshold}$. The maximum horizontal force might come from the net slab pull force, F_{NSP} , arising from an active neighboring subduction zone. F_{NSP}

corresponds to the fraction of the weight exerted by the slab negative buoyancy (F_b) that is actually available to act on the trailing plate. The negative buoyancy of a subducting slab may result in a force higher than the ridge push by at least one order of magnitude (hence, $\sim 2 \times 10^{13}$ N/m, ?). The ratio F_{NSP}/F_b would be lower than 0.5 (?) or on the contrary, higher than 0.7 (?). The maximum force available to drive subduction initiation has been moreover advocated to be limited to 10^{13} N/m (?). To take into account the possible F_{NSP} interval, we choose to considerer a first threshold $F_1^{\text{threshold}} = 10^{13}$ N/m and a higher one $F_2^{\text{threshold}} = 1.5 \times 10^{13}$ N/m.

We compare the evolution of F_{res} through time, t , to the considered threshold $F_i^{\text{threshold}}$ (see for instance Fig. 3-1c,2c), by computing 3 quantities: (1) $F_{\text{res}}^{\text{mean}vt}$ is the F_{res} mean computed over the whole simulation duration. If $F_{\text{res}}^{\text{mean}vt}$ exceeds the chosen threshold, then we compute (2) the time span Δt_{excess} over which F_{res} exceeds the limit, and (3) $F_{\text{res}}^{\text{excess mean}}$ that is the average value of F_{res} over the interval Δt_{excess} (Fig. S5). The quantities $F_{\text{res}}^{\text{mean}vt}$, the beginning and end of the Δt_{excess} interval, and $F_{\text{res}}^{\text{excess mean}}$ are given in Table S2 for all experiments.

The global evolution of the horizontal compressive stresses acting on the lithospheres is considered as realistic ('admis.' in Table S2) if :

- F_{res} is always $< F_i^{\text{threshold}}$, which is often obtained when $F_{\text{res}}^{\text{mean}vt}$ is significantly lower than $< F_i^{\text{threshold}}$ (Fig. S5a1),
- or F_{res} is most of the time $< F_i^{\text{threshold}}$, and, when $F_i^{\text{threshold}}$ is exceeded, if the duration Δt_{excess} is short (<2.5 Myr) and if $F_{\text{res}}^{\text{excess mean}}$ does not exceed $F_i^{\text{threshold}}$ by more than 1×10^{12} N/m (Fig. S5a2).

The simulated evolution of $F_{\text{res}}(t)$ is considered as leading to an excessive compression that is not realistic ('too cp') if:

- Compressive stresses are always, or soon after the convergence start, exceeding the threshold (Fig. S5b1, left). This is observed in most cases of absence of localization at the fault gouge ('NL' in Table S2);
- or if $\Delta t_{\text{excess}} > 2.5$ Myr and/or if $F_{\text{res}}^{\text{excess mean}}$ exceeds the threshold by more than 1×10^{12} N/m (Fig. S5b1, right).

In some experiments, the modeled F_{res} force remains below the chosen admissible threshold until a significant time (approximately between 5 and 10 Myr), before a rise leading a extreme value exceeding the threshold during a long time span ($\Delta t_{\text{excess}} \gg 2.5$ Myr, Fig. S5b2). We observe that this time window and stage of convergence accommodation roughly corresponds to second stage of subduction initiation defined by ?, namely the 'incipient-localized stage' corresponding to the end of the convergence localization at the infant subduction plane. In such a case, one may assume that the process of subduction initiation modeled in the experiment would then cease. Since the subduction initiation would fail, these simulations are classified as 'too cp', but in details, one could consider that the very first stages could still have occurred, before the subduction aborts during or at the end of the incipient-localized stage. These experiments are denoted with an asterisk in Table S2.

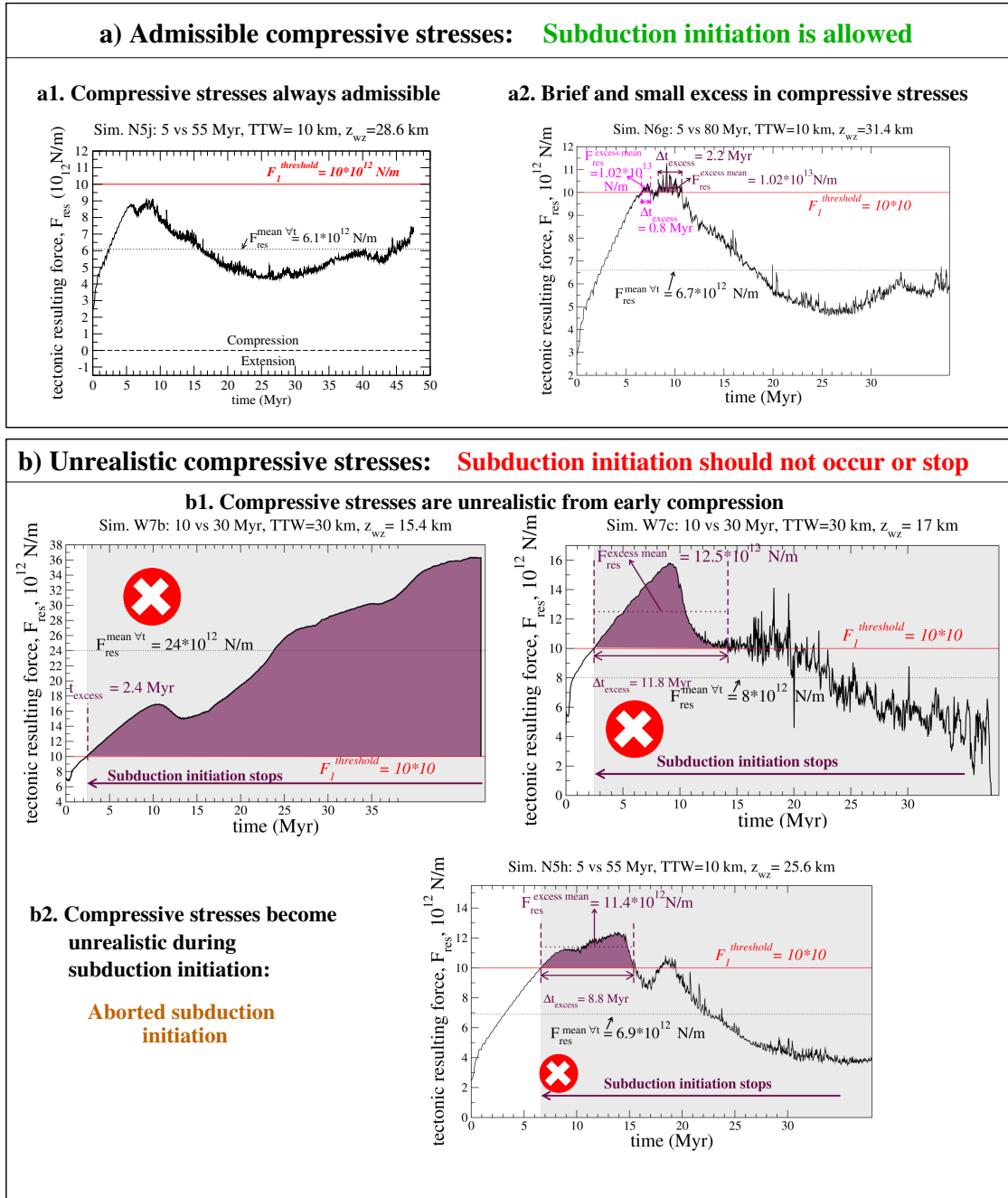


Figure S5: Resulting tectonic force evolution through time, $F_{\text{res}}(t)$ and comparison to the admissible threshold. Panel (a) the $F_{\text{res}}^{\text{threshold}}$ threshold for the horizontal compressive force is never (a1) or hardly exceeded (a2). Panel (b) The simulated F_{res} significantly exceeds the compression threshold. Subduction initiation does not occur (b1), or prematurely stops (b2, aborted subduction initiation).

S3. Analysis of the OP subduction process

OP subduction is modeled for plate age pairs of Group Low defined in Fig. 5 and section 4.1 ($\Delta A/A_y \leq 1$), and, to a lesser extent, of Group Moderate ($1 < \Delta A/A_y < 4.5$). We detail in the following (1) the characteristics of these 2 groups, (2) how heat dissipation peaks at the depth of the brittle-ductile transition of the YP during the OP underthrusting, and (3) how boundaries of this regime may be controlled.

(1) In Group Low the plate strength contrast is moderately low, both plates have roughly similar capacity to subduct and the subduction zone polarity is selected as a function of the fault gouge depth. Convergence localization at the fault gouge can be very fast, as mainly observed for young lithospheres (such as for sim. 5vs10, Fig. 1a). Since both plates are quite thin, the fault gouge bound for subduction initiation is relatively shallow. Alternatively, for thicker plates composing Group Low, the first stage of convergence is longer, whatever the subduction polarity, which enhances plate buckling and deformation before localization at the embryonic subduction plane occurs (20vs30 Myr, Fig. 2 row 2). This lasting first stage of diffuse deformation fosters the fault gouge burying prior to localization. Hence the minimum z_{wz} ensuing OP subduction does not need to be initially deep in Group Low (only 12 km, Fig. 4a), and is close to the initial Moho depth (8.3 km). This could explain that the shallowest z_{wz} ensuing OP subduction is initially very low in Group Low (12 km, Fig. 4a), and close to the initial Moho depth (8.3 km). Group Moderate constitutes a midway pattern between Groups Low and High. The mode of convergence accommodation is more sensitive to the whole structural setup, particularly to the TTW. Even if the YP deforms more easily than the OP, the OP can also accommodate an important amount of convergence before the subduction plane formation. By the way, in Group Moderate the YP can be moderately thick with respect to the OP, so when YP subduction is triggered (1) it buckles at long wavelengths, which shifts the forming subduction plane away from the initial fault zone (by 50 to 100 km for 20vs55, sim. N11e and sim. W11e-i, Table S2) and implies longer duration, (2) it bends with high curvature radius (low dip angle). This is also observed for higher $\Delta A/A_y$, up to 4.5 (15vs80, simulations W9d-f, and 10vs55, simulations W8m,n, Table S2).

(2) Compared to the process of YP subduction discussed in section 4.3, we observe the same concomitant evolutions for F_{res} and the incipient subduction plane development in the case of OP underthrusting, the depth of maximum resistance that has to be achieved being z_{BDT}^{YP} . In Simulation N10g (20vs30 Myr, TTW = 10 km, $z_{wz} = 26.3$ km, Fig. 3-2a,c, Section S3). the maximum in F_{res} is met at 9.1 Myr, while at 10.3 Myr the bottom of the weak fault gouge reaches ~ 21.3 km depth, which is the computed z_{BDT} for a lithospheric age of 30 Myr, close to the YP age at this time. The 600°C YP isotherm is rising up to ~ 21 km depth, revealing a high localized shear heating. The depth z_{BDT}^{YP} is hence a key depth for OP subduction initiation. Moreover, we find that for the plate age pairs of Group Moderate ($1 < \Delta A/A_y < 4.5$) OP subduction is modeled for both TTWs when z_{wz} at convergence onset is approximately equal to z_{BDT}^{YP} (Fig. 4b and S4). It is not the case for Group Low ($\Delta A/A_y \leq 1$), for which OP subduction is obtained for fault gouge depths barely deeper than the Moho depth (see above). We still observe for Group Low that a significant shear heating within or close to the incipient subduction channel is also released at depths corresponding to the temperature range 500-650°C.

(3) We note that the two ranges of $\Delta A/A_y$ showing OPS are discontinuous (Fig. 4a and S4). For the plate age pair in between, 2vs5 ($\Delta A/A_y = 1.5$), no clear OP subduction is modeled (only

delayed, secondary OP subduction or DSubduction, Simulations N1c-d and W1c, Table S2). In such a setting where the two lithospheres are particularly thin, we hypothesize that the z_{wz} interval that would yield OP subduction is possibly very narrow, and cannot be matched without strongly refining the numerical mesh. We speculate that experiments based on the same $\Delta A/A_y$ but simulating thicker lithospheres (8vs20 Myr for instance) would result in OP subduction for $z_{wz}/z_{TT} \sim 0.25$ (Fig. 5). Similarly, the same procedure could lightly extend beyond $\Delta A/A_y = 2$ the interval of plate age pairs showing OP subduction.

S4. Failure of convergence localization while z_{wz} is very deep - Influence of TTW

As mentioned in sections 3.2 and 3.3 a wide thermal transition can promote subduction initiation, but the underlying reason is unclear. For the plate pairs 15vs80 and 20 vs55 Myr showing mainly subduction failure when $TTW = 10$ km, the amplitude of YP buckling is slightly emphasized (by ~ 1 km) near the fault gouge in relation to the rest of the lithosphere when $TTW = 30$ km, whereas this enhancement occurs on the contrary close to the left-hand kinematic boundary when $TTW = 10$ km. Note that for these two plate age pairs, the YP is rather thick, and is buckling with a long wavelength. We assume that for these two plate age pairs the initial fault gouge when $TTW = 10$ km may be misplaced at convergence start with respect to the spatial and vertical oscillations of the Moho associated with YP buckling (for instance close to an uplift maximum), preventing the formation of a down-dip shear plane. In contrast the facilitating effect obtained when $TTW = 30$ km that enhances vertical YP deformations near the fault gouge might come from the enlarging of the space available for YP folding. This slight deformation increase might be sufficient to further favor convergence localization at the fault gouge. Furthermore, we note that the widening of the thermal transition yields slightly colder temperature on the YP side and warmer temperatures on the OP side. This light warming close to the fault gouge on its OP side when TTW is increased to 30 km might yield there a local weakening and further promote YP subduction.

S5. Long-term evolution of the tectonic force, F_{res}

We focus on the stress state modeled in our experiments after the peak in compression, up to the simulation end, when the length of the incoming plate is maximum (roughly equal to or exceeding 400 km-length). The last part of our experiments might be compared to a classical stage where the subduction zone has almost reached self-sustainment (i.e., for slab length longer than ~ 250 km, ?). Simulations W7e (10vs30, $TTW = 30$ km, $z_{wz} = 22.0$ km) and W10f (20vs30, $TTW = 30$ km, $z_{wz} = 25$ km) presented in Fig. 3b,c are used as case-studies.

The first part of the tectonic force evolution, is detailed in section 4.3, where we observe that the maximum in compression is reached when almost all the convergence is localized along the nascent subduction plane (Fig. S6c, point 1). This occurs when the depth of the incipient subduction plane is approximately close to the brittle-ductile transition within the overlapping plate. Once the weak layer forming the proto-subduction interface has reached this depth, compression decreases. It corresponds to a significant decrease in the tectonic force F_{res} , between ~ 14 and 20 Ma (Fig. S6c, point 2). At this time the new incoming plate tip has reached a ~ 110 km depth and is entering the asthenosphere. This starts activating two small-scale convection cells in the hot mantle on both sides of the forming downgoing slab (Fig. S6a and b, point 2). Vertical speeds at the slab tip and in the underneath asthenosphere are strongly enhanced, up to 7 cm/yr. From that

time, the asthenosphere flows are progressively activated downwards from the base of both converging plates. We observe that the mantle dragging by the plate motion fosters the subduction process and decreases the compressive stresses necessary to sustain convergence at constant rate (Fig. S6c, points 2 to 3). The compression lowering then goes on from \sim 22 to \sim 38 Ma, when the slab tip reaches 265 km-depth, after a 380 km-long convergence. This continuous decrease likely results from the slab pull rise up. At the end of the simulation, the 2 "conjugate" convective cells are strongly horizontally elongated, locally disturbed by vertical downward flows resulting from dripping from the unstable sub-lithospheric layer.

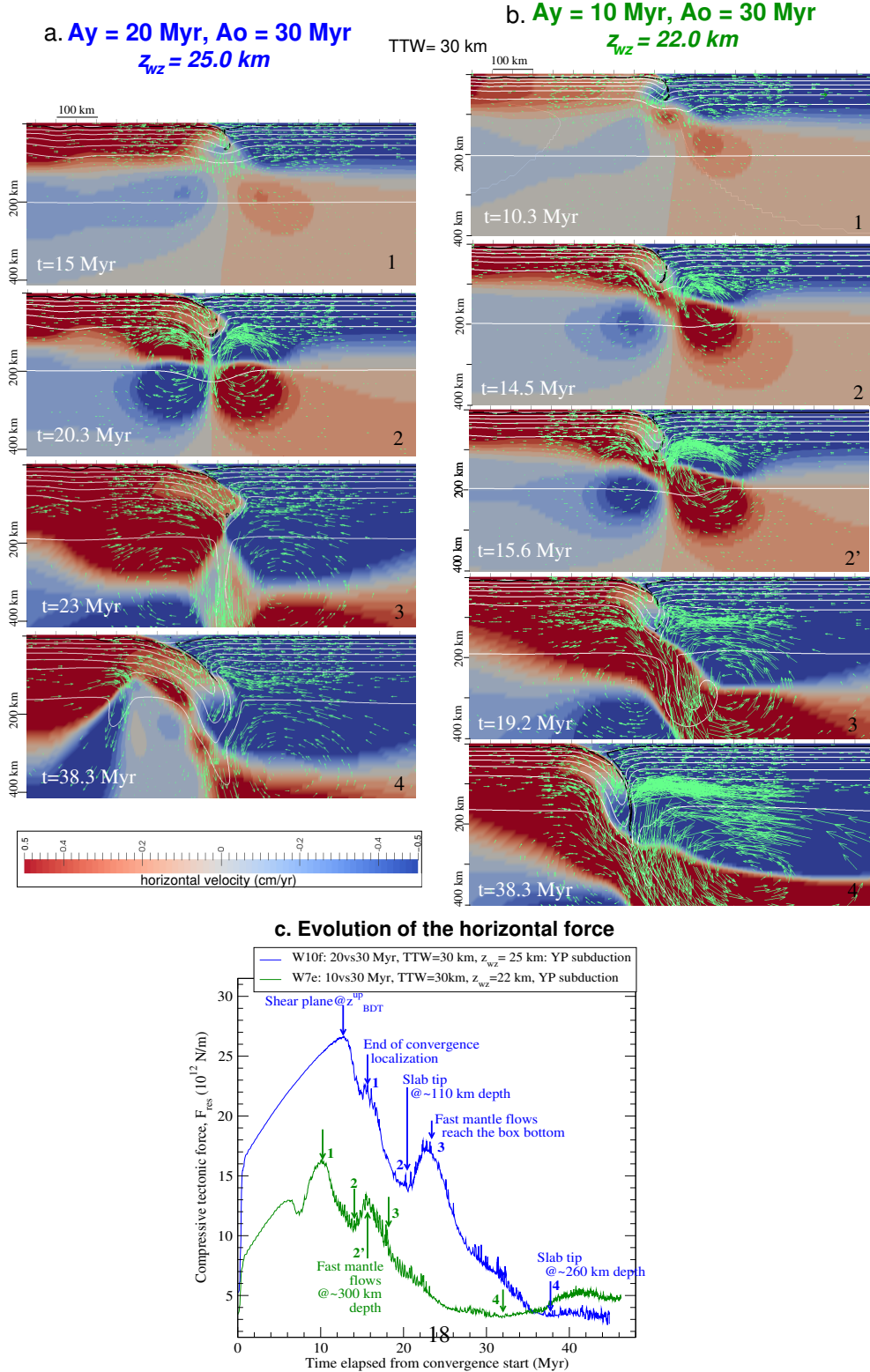


Figure S6: Evolution of the subduction zone once convergence is localized on the incipient subduction plane, for simulation (a) W10f and (b) W7. The color scale used to map the horizontal velocity is saturated to -0.5 and +0.5 cm/yr to highlight slow motions, while the total speed is depicted through green vectors. (c) Evolution of the resulting tectonic force, F_{res} , for the simulations displayed in panels a (blue) and b (green).

S6. Additional experiments, investigating different rheologies

Table S3: Extra simulation list. See below for abbreviation definition.
(continued on next page)

Run	A_y vs A_o (Ma)	ΔA \bar{A}_y - Ma)	TTW (km)	z_{wz} (km)	Mantle brittle coeff., γ_m	Crust rheology γ_c/E_a^c (kJ.mol $^{-1}$)	Gouge rheology γ_{TF}/E_a^{TF} (kJ.mol $^{-1}$)	Result
wTF1	5vs80	15	10	12.3	1.6	0.05/360	0.0005/220	NL
wTF2	5vs80	15	10	32	1.6	0.05/360	0.0005/220	NL
wTF3	5vs30	5	10	12.3	1.6	0.05/360	0.0005/220	NL
wTF4	5vs30	10	10	24	1.6	0.05/360	0.0005/220	NL
wTF5	5vs55	10	10	12.3	1.6	0.05/360	0.0005/220	NL
wTF6	5vs55	10	10	27	1.6	0.05/360	0.0005/220	NL
OC1-1592	10vs30	2	0	16.4	1.6	0.05/360	crust rheol.	NL
OC1bis-1593	10vs30	2	0	22.5	1.6	0.05/360	crust rheol.	NL
OC2-1594	10vs30	2	0	25	1.6	0.05/360	crust rheol.	YPs
wOC1-1574	10vs30	2	0	16.4	1.6	0.01/245	crust rheol.	OPs
wOC3-1618	10vs30	2	0	12.3	1.6	0.01/245	crust rheol.	Double S
OC3-?	5vs30	5	0	10.4	1.6	0.05/360	crust rheol.	NL
OC3-1582	5vs30	5	0	12.3	1.6	0.05/360	crust rheol.	NL
OC3-1586	5vs30	5	0	17.2	1.6	0.05/360	crust rheol.	YPs
OC3-1579?	5vs30	5	0	20.5	1.6	0.05/360	crust rheol.	YPs
wOC4-?	5vs30	5	0	10.4	1.6	0.01/245	crust rheol.	Double S
wOC?-	5vs30	5	0	12.3	1.6	0.01/245	crust rheol.	YPs
wOC?-	5vs30	5	0	17.2	1.6	0.01/245	crust rheol.	YPs
wOC4-1569	5vs30	5	0	20.5	1.6	0.01/245	crust rheol.	YPs then Double S
wOC?	5vs30	5	0	24	1.6	0.01/245	crust rheol.	YPs
wOC5	5vs30	5	0	10.4	1.6	0.01/245	crust rheol.	Double S
wOC6bis-1552	5vs30	5	0	12.3	1.6	0.01/245	crust rheol.	NL mais -380 kg/m 3
wOC6-1573	5vs30	5	0	12.3	1.6	0.01/245	crust rheol.	YPs
OC4	5vs55	10	0	12.3	1.6	0.05/360	crust rheol.	NL
OC4i-1605	5vs55	10	0	24	1.6	0.05/360	crust rheol.	NL
OC4ii-1606	5vs55	10	0	32	1.6	0.05/360	crust rheol.	NL mais pb xpstart
OC4iii-1607	5vs55	10	0	40	1.6	0.05/360	crust rheol.	YPs secondaire
OC4iv-1608	5vs55	10	0	48	1.6	0.05/360	crust rheol.	YPs secondaire
OC4v-1728	5vs55	10	0	56	1.6	0.05/360	crust rheol.	YPs

continued on the next page...

...continued

Run	A_y vs A_o	$\Delta A/A_y$	TTW	z_{wz}	γ_m	Oc. crust	Gouge	Result
wOC7-1620	5vs55	10	10	12.3	1.6	0.01/245	crust rheol.	YPs then OPs
wOC8-1609	5vs55	10	0	16.4	1.6	0.01/245	crust rheol.	NL
wOC8bis-1610	5vs55	10	0	20	1.6	0.01/245	crust rheol.	YPs
wOC9-1611	5vs55	10	0	24	1.6	0.01/245	crust rheol.	YPs
wOC9-1612	5vs55	10	0	32	1.6	0.01/245	crust rheol.	YPs
wOC9-1613	5vs55	10	0	40	1.6	0.01/245	crust rheol.	YPs
wOC9-1620	5vs55	10	0	48	1.6	0.01/245	crust rheol.	YPs
OC7-1637	5vs80	15	0	12.3	1.6	0.05/360	crust rheol.	NL
OC7-1623	5vs80	15	0	16.4	1.6	0.05/360	crust rheol.	NL
OC7-1624	5vs80	15	0	20	1.6	0.05/360	crust rheol.	NL
OC7-1627	5vs80	15	0	32	1.6	0.05/360	crust rheol.	YPs secondaire
OC7-1628	5vs80	15	0	40	1.6	0.05/360	crust rheol.	YPs secondaire
OCT-1629-1729	5vs80	15	0	48	1.6	0.05/360	crust rheol.	YPs secondaire
wOC10-1638	5vs80	15	0	12.3	1.6	0.01/245	crust rheol.	3 successive YPs
wOC11-1630	5vs80	15	0	16.4	1.6	0.05/360	crust rheol.	NL
wOC12-1631	5vs80	15	0	20	1.6	0.05/360	crust rheol.	NL
wOC13-1632	5vs80	15	0	24	1.6	0.01/245	crust rheol.	YPs
wOC14-1634	5vs80	15	0	32	1.6	0.01/245	crust rheol.	YPs
wOC15-1635	5vs80	15	0	40	1.6	0.01/245	crust rheol.	YPs
wOC16-1636	5vs80	15	0	48	1.6	0.01/245	crust rheol.	YPs
wM1	5vs55	10	10	27.1	0.8	0.05/360	crust rheol.	NL
wM2	5vs55	10	10	27.1	0.45	0.05/360	crust rheol.	NL
wM3	5vs55	10	10	13.5	0.45	0.05/360	crust rheol.	NL
wM4	5vs55	10	10	28.5	0.45	0.05/360	crust rheol.	NL
wMOC1	5vs55	10	10	32	0.45	0.005/220	crust rheol.	repeated short-lasting YPs
wM3	5vs55	10	10	13.5	0.45	0.05/360	crust rheol.	NL
vwM1	5vs55	10	10	13.5	0.3	0.05/360	crust rheol.	NL
vwM2	5vs55	10	10	28.5	0.3	0.05/360	crust rheol.	NL
vwMOC1	5vs55	10	10	32	0.3	0.005/220	crust rheol.	aborted OPs
vwMOC2	5vs55	10	10	32	0.3	0.0005/220	crust rheol.	OPs
vwMOC3	5vs80	15	10	32	0.3	0.001/220	crust rheol.	OPs
vwMOC4	5vs80	15	10	32	0.3	0.0005/220	0.05/360	NL

Most abbreviations are defined in Table S2 caption, the other abbreviations are: OC: oceanic crust. TF: transform fault gouge. M: Mantle. Prefix 'w': weak, and 'vw': very weak. 'crust rheol.' means that the fault gouge rheology is set to the crust rheology for the same experiment.